Received: 6 February 2024 | Accepted: 19 February 2024

DOI: 10.1111/srt.13654

ORIGINAL ARTICLE

WILEY

Correlation analysis between texture features and elasticity of skin hyperspectral images in the near-infrared band

Juhyun Kim[1] | **Onseok Lee**[1,2]

[1]Department of Software Convergence, Graduate School, Soonchunhyang University, Asan City, Chungnam, Republic of Korea

[2]Department of Medical IT Engineering, College of Medical Sciences, Soonchunhyang University, Asan City, Chungnam, Republic of Korea

Correspondence
Onseok Lee, Department of Medical IT Engineering, College of Medical Sciences, Soonchunhyang University, 22, Soonchunhyang-ro, Asan city, Chungnam 31538, Republic of Korea.
Email: leeos@sch.ac.kr

Funding information
Soonchunhyang University Research Fund; BK21 FOUR (Fostering Outstanding Universities for Research), Grant/Award Number: 5199990914048; National Research Foundation of Korea (NRF) grant funded by the Korea government (MSIT), Grant/Award Number: 2022R1A2C1010170; Health Fellowship Foundation, Grant/Award Number: 2023

Abstract

Background/purpose: Skin elasticity was used to evaluate healthy and diseased skin. Correlation analysis between image texture characteristics and skin elasticity was performed to study the feasibility of assessing skin elasticity using a non-contact method.

Materials and methods: Skin images in the near-infrared band were acquired using a hyperspectral camera, and skin elasticity was obtained using a skin elastimeter. Texture features of the mean, standard deviation, entropy, contrast, correlation, homogeneity, and energy were extracted from the acquired skin images, and a correlation analysis with skin elasticity was performed.

Results: The texture features, and skin elasticity of skin images in the near-infrared band had the highest correlation on the side of eye and under of arm, and the mean and correlation were features of texture suitable for distinguishing skin elasticity according to the body part.

Conclusion: In this study, we performed elasticity and correlation analyses for various body parts using the texture characteristics of skin hyperspectral images in the near-infrared band, confirming a significant correlation in some body parts. It is expected that this will be used as a cornerstone of skin elasticity evaluation research using non-contact methods.

KEYWORDS
correlation analysis, hyperspectral imaging, NIR, noncontact, skin elasticity, texture analysis

1 | INTRODUCTION

Human skin is an essential organ for overall body homeostasis, and aging occurs owing to internal and external body factors, which can be confirmed with the naked eye. Skin aging reduces the skin regeneration ability and is accompanied by an increase in aging cells, likely leading to various pathological outcomes.[1,2] Therefore, there is an increasing need to develop technology to observe skin aging characteristics to maintain healthy skin and prevent skin diseases. As such, anti-aging is receiving attention as a major interest worldwide, and research on skin aging prevention and management is increasing the skin, an essential external organ of the body.[3]

The skin comprises three major layers: the epidermis, dermis, and subcutaneous fat. The characteristics and types of materials that make up each layer are different.[4,5] In addition, the skin has mechanical properties that are affected by deformability, such as

anisotropy and viscoelasticity. The skin affected by physical and chemical deformation from the outside and inside becomes dry, wrinkles deepen, and elasticity decreases owing to a decrease in moisture, the phenomenon appears.[6] Such changes resulting from skin elasticity deformation, appear to be related to pathological changes. Aging is an example of a pathological change in the skin. Because the most noticeable feature is a decrease in skin elasticity as the skin ages, measuring skin elasticity is an important indicator for assessing skin aging.

Among the three layers of the skin, skin elasticity is influenced by type I collagen in the dermis layer, which accounts for about 90% of the skin's weight, and the elasticity of the dermis layer is determined by the composition and density of elastin and collagen fibers that make up the dermis layer.[7] Therefore, to evaluate skin elasticity, it is important to analyze the elasticity value of the dermis layer, which is deeper than the skin epidermis, to evaluate skin aging and skin condition.

Devices based on a suction method that directly contacts the measuring device with the skin are widely used for measuring skin elasticity.[8,9] These devices require specialized knowledge to interpret the measurement results. The principle of elasticity measurement, which applies a suction method that creates temporary deformation by contact with the skin, can cause damage in the case of skin weakened by disease.[10] Therefore, it is necessary to go beyond noninvasive and noncontact skin evaluation methods when measuring skin characteristics.

There is increasing demand for optical-based imaging technology as a noninvasive and noncontact method for measuring the elasticity of the dermal layer of the skin. Images using a general digital camera can observe the skin's surface through the visible light band required for naked eye observation among the light spectrum region. However, to obtain information on the dermal layer area, directly related to skin elasticity, skin observation information corresponding to the near-infrared region, a wavelength range that can penetrate deeper than the skin surface, is required.[11,12] However, a separate system is required to interpret the image information to collect elasticity information of the dermal layer through optical images.

The hyperspectral imaging system, a recent noninvasive spectroscopy technology for skin evaluation, includes spectral bands other than visible light; therefore, in vivo, characteristics that cannot be seen in visible light are objectively identified through indicators such as spectral reflectance data. This method has been proposed as a promising technology.[13,14] Irregular curvatures and wrinkles form on the skin's surface depending on the collagen and elastin structure in the dermal layers.[6] The depth, uniformity, and distribution of wrinkles formed on the skin can be analyzed using skin's texture characteristics.[15] Therefore, we attempted to obtain information on skin wrinkles and evaluate skin elasticity using the image texture characteristics of the near-infrared band, which can be used to obtain information about the dermis layer from hyperspectral images.

In this study, we aimed to analyze the relationship between skin elasticity and the characteristics of the dermal layer of the skin, not just the visually observable outer surface of the skin. We performed a correlation analysis between the texture characteristics of skin images corresponding to the near-infrared region and the measured elasticity, rather than limiting ourselves to the reflectance information used in studies using existing hyperspectral images.

2 | MATERIALS AND METHODS

2.1 | Participants

The experimental participants in this study consisted of 17 healthy Korean men, 7 men, and 10 women, aged 20 to 44 years (26.59 ± 6.28, mean ± standard deviation). The test participants had no serious medical histories or skin diseases. The participants did not apply cosmetic products to their skin until 4 h before the experiment, wiped the observed area with an alcohol swab and dried the moisture.

2.2 | Measurement

2.2.1 | Definition of elasticity in this study

"Elasticity," as defined in this study, is the force required to press the skin when pressed inward.[16] Therefore, the harder the skin, the higher its resistance, which requires a large force to deform, resulting in a high elasticity value.

2.2.2 | Observation location

In this study, 10 body parts were selected for observation to analyze the correlation between features based on hyperspectral images and evaluate elasticity according to various anatomical parts of the body (Figure 1).

2.2.3 | Measurement of skin elasticity

This study measured skin elasticity using a skin elastimeter (Delfin, Kuopio, Finland).[16,17] A skin elastimeter measures the value (N/m) per unit area in which the indenter of the device is in contact with the skin. When the indenter at the center of a 23 mm diameter plate was manually pressed into the skin for approximately 2 s, with the participant lying comfortably on a mat, the instantaneous force required to deform the skin was measured. The magnitude of the force measured at this time is called the intense skin elasticity (ISE). Therefore, when the indenter of the device contacts the skin, the higher the hardness of the skin, and the more force the indenter needs to deform the skin, the higher the ISE value (N/m). When the indenter of this device lightly touched the five times (approximately 0.5 s), the average elasticity value (N/m) was recorded on the device's LED board. Finally, the elasticity value used in this study was obtained by values for the same body part and then using the average of the elasticity values measured three times.

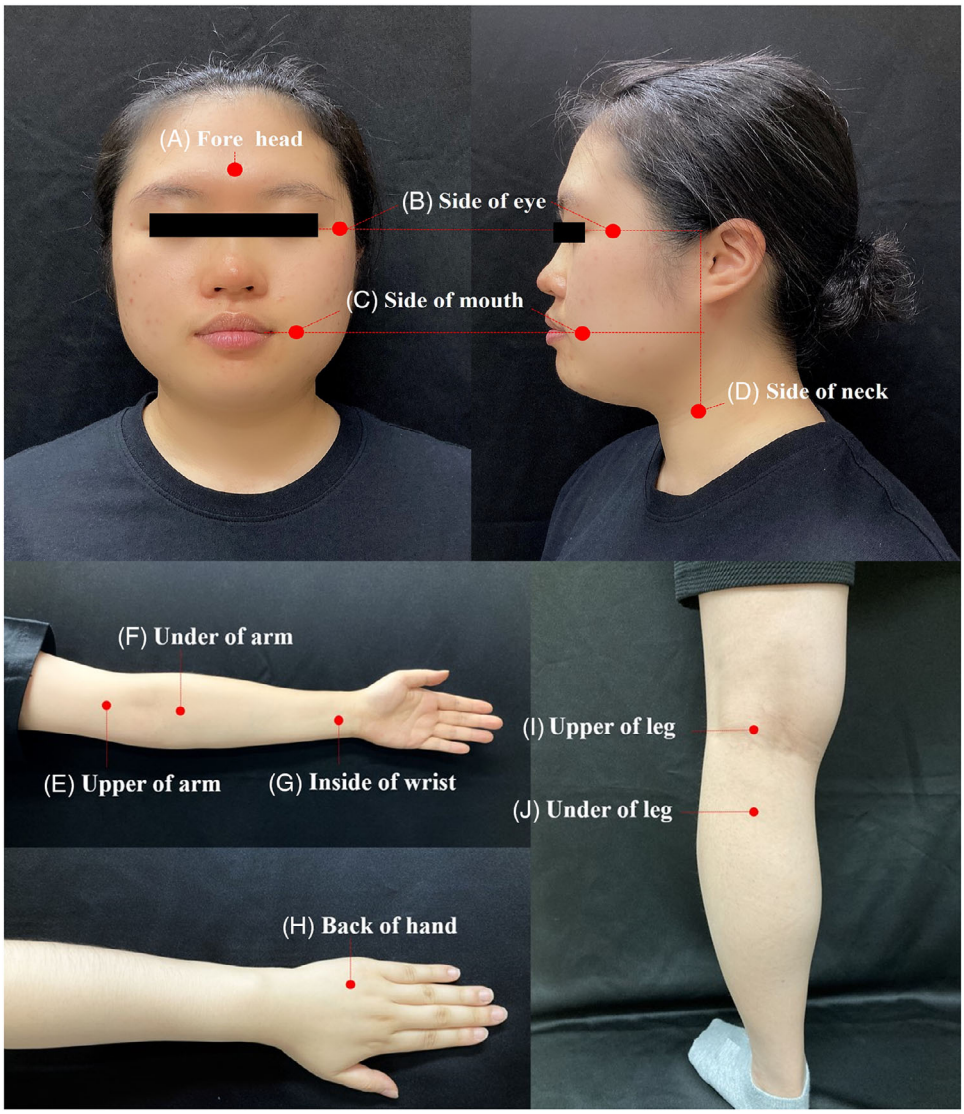

FIGURE 1 Images of observed body parts. (A) Forehead, (B) side of eye, (C) side of mouth, (D) side of neck, (E) upper of arm, (F) under of arm, (G) inside of wrist, (H) back of hand. (I) upper of leg, (J) under of leg.

2.2.4 | Acquisition of skin hyperspectral imaging and ROI

This study acquired skin hyperspectral images to analyze various characteristics of the dermis layer's near-infrared wavelength images involved in skin elasticity. The device was used to capture the images was the SNAPSACAN Hyperspectral Camera (IMEC, Leuven, Belgium). This device can acquire images in the visible and NIR wavelength ranges with 150 spectral bands and records them using the snap-scan method. A Tamron 60 mm macro lens (Tamron, SP AF 60 mm F2 Di II IF LD Macro 1:1, Japan) was used. The lighting used for filming was a 650 W halogen lamp H-1000 (FOMEX, Seoul, Republic of Korea) with a light reflector, and the participants wore light-blocking goggles to protect their eyes from the light source. While photographing the skin, the participants sat on a chair or stood comfortably. The distance between the skin and the camera lens was 50 cm. The camera was fixed horizontally to the participants, and the light was set at a 45° angle above the participants. The photographed areas were 10 per participant, the same as when measuring elasticity. The imaging time was 17–20 ms skin sample. The shooting environment was a light-blocked dark room with only halogen lighting to prevent the influence of ambient light on the hyperspectral images. After obtaining the skin image, a white reference with a reflectance of 95% was obtained to control lighting unevenness. The hyperspectral image was obtained as a processed image in a preprocessed state in the Snapscan Application linked to the camera using a dark reference and white reference.

The initially acquired hyperspectral image of the skin measured 1,024 × 1,024 pixels. When acquiring images, light reflections and shadows owing to the curves of body parts are mainly created in the outer areas of the image. Therefore, skin areas unaffected by reflections and shadows were randomly cropped to four per skin sample in the image. When cropping the image for the region of interest (ROI),

it was set to 378 × 378 pixels, corresponding to 10 × 10 mm, which is smaller than the 23 mm plate diameter of the skin elastimeter used to measure the image elasticity value, and a total of 1,292 images were acquired.

2.3 | Analysis of data

This study aimed to analyze the correlation between the texture characteristics of deep skin layers and skin elasticity obtained from hyperspectral images in the near-infrared band corresponding to 750–900 nm.[18,19] Therefore, this section introduces the texture features analyzed as evaluation features of elasticity in this study and the statistical analysis used.

2.3.1 | Texture features

The texture features analyzed in this study were extracted by quantifying intuitive texture expressions such as rough, smooth, or bumpy as functions representing spatial changes in pixel brightness. The texture features used were the statistical values of the image pixels (mean, standard deviation [std], entropy) and gray-level co-occurrence matrix (GLCM).[20] GLCM calculates the correlation between an image's pixel features and defines the image's texture characteristics through information about the relationship between the surrounding pixels. In this study, contrast, correlation, homogeneity, and energy features were used in this study. The formula for calculating each statistic are as follows: In the formula below, N is the number of pixels corresponding to the width and height of the image, A is a matrix with pixel values of the image, and i and j represent the matrix positions corresponding to the width and height in A. μ in Equation (5) is the result of Equation (1), and σ is the result of Equation (2).

1. Mean

$$\mu = \frac{1}{N}\sum_{i=1}^{N}\sum_{j=1}^{N} A(i,j) \tag{1}$$

2. Standard deviation

$$\mathrm{ff} = \frac{1}{N}\sum_{i=1}^{N}\sum_{j=1}^{N} A\left(i-\mu_i, j-\mu_j\right) \tag{2}$$

3. Entropy

$$-\frac{1}{N}\sum_{i=1}^{N}\sum_{j=1}^{N} A(i,j)\,\log A(i,j) \tag{3}$$

4. Contrast

$$\sum_{i=1}^{N}\sum_{j=1}^{N} (i-j)^2 A(i-j) \tag{4}$$

5. Correlation

$$\sum_{i=1}^{N}\sum_{j=1}^{N} \frac{(i-\mu_i)(j-\mu_j)}{\sigma_i\sigma_j} \tag{5}$$

6. Homogeneity

$$\sum_{i=1}^{N}\sum_{j=1}^{N} \frac{A(i,j)}{1+|i-j|} \tag{6}$$

7. Energy

$$\sum_{i=1}^{N}\sum_{j=1}^{N} A(i,j)^2 \tag{7}$$

2.3.2 | Analysis of correlation

In this study, we attempted to objectify the skin elasticity evaluation index by performing a correlation analysis between texture features and elasticity extracted from skin hyperspectral images in the near-infrared band and selecting image features that were significantly correlated with skin elasticity. Pearson's correlation analysis was used as the data to be analyzed had a bivariate normal distribution. As a result of the analysis, the correlation coefficient r represents the slope of the linearity between the two variables. The correlation coefficient has a value between $-1 < r < 1$. If r is less than zero, the two variables are interpreted as having a negative correlation; if r is greater than zero, the two variables are interpreted as having a negative correlation. A significance test of the correlation coefficient was performed, and values were considered significant at $p < 0.05$.

2.3.3 | Analysis of ANOVA

An analysis of variance (ANOVA) was performed for each feature to select the optimal image texture features by determining whether the seven texture features extracted from the hyperspectral images in the near-infrared band significantly differentiated the elasticity of different body parts. However, because ANOVA analysis could not reveal specific differences between the groups, the Scheffe method was performed for post-hoc test to analyze the differences between body part groups for each texture feature. Figure 2 shows a diagram showing the flow chart of the overall analysis procedure.

2.3.4 | Environment of data analysis

The texture feature extraction described in Section 2.3.1 was performed using MATLAB 2021b (The MathWorks, Inc., Natick, MA, USA). Statistical analyses in 2.3.2 and 2.3.3 were performed using SPSS version 25.0 (SPSS Inc, Chicago, IL, USA).

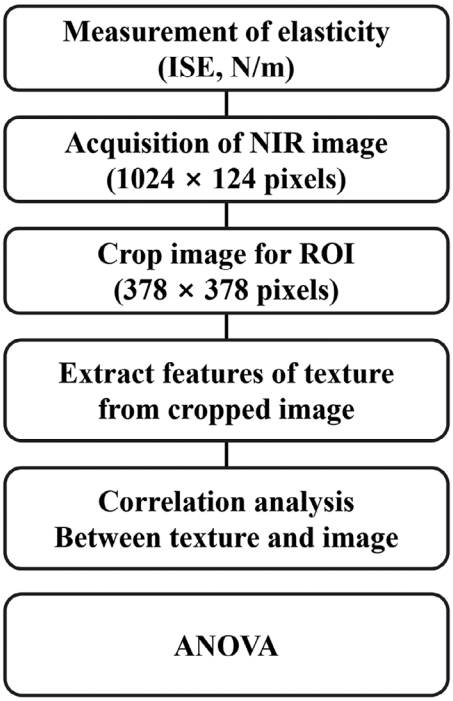

FIGURE 2 Experimental sequence image.

2.4 | Ethics

To conduct this study, the research protocol was approved by the Ethics Committee of Soonchunhyang University. (IRB number: 202303-SB-019-03) Written consent was provided and consent was obtained from all experimental participants. In addition, a sufficient explanation of the research method was provided before the experiment to ensure participants were familiar with the method.

3 | RESULTS

3.1 | Comparison of elasticity values according to body part

Elasticity statistics were compared for 1292 skin samples. Figure 3 shows the mean, standard deviation, median value, and data distribution for elasticity by body part. The average elasticity value in all parts was normal at the $p < 0.05$ level. The mean elasticity was highest under of legs and lowest on side of neck. The elasticity std was highest in upper of leg and lowest on side of neck. The elasticity's median, like mean, was highest in upper of leg.

3.2 | Correlation analysis of elasticity and texture characteristics according to body part

In Table 1, according to the correlation analysis and significance test between the elasticity value for each body part and the texture characteristics of the image in the NIR band, if the correlation coefficient is significant at $p < 0.05$ level, it is denoted as *Y*, and if it is not significant, it is denoted as *N*. If the correlation coefficient is significant, it is indicated as (+) if there is a positive correlation and (−) if there is a negative correlation. Overall, the side of eye, under of arm, and under of leg areas had a significant correlation between texture characteristics and elasticity in the NIR band.

In the case of mean, side of eye and upper of leg had a significant positive correlation $p < 0.05$, and upper of arm, under of arm, inside of wrist, and upper of leg had a negative correlation. In entropy, there was a significant positive correlation $p < 0.05$ level in forehead, side of eye, side of mouth, and under of leg, and a significant negative correlation in upper of arm and under of arm. Regarding correlation, side of eye, side of mouth, side of neck, and under of leg had a significant positive correlation at $p < 0.05$, and under of arm had a significant negative correlation at $p < 0.05$ level.

3.3 | ANOVA analysis by region for each feature

In Figure 4, an ANOVA analysis was performed to determine whether each texture feature could evaluate significant differences in skin elasticity depending on the body part. Subsequently, through a post-hoc test, the network structure was used to determine whether each texture feature significantly differed in average elasticity between body parts. The observed texture features were categorized as (a)−(g). Each point shown in the image of this network structure represents a different body part, and the line segment connecting the points for the two parts represents a relationship in which the corresponding texture feature does not show a significant difference in the average skin elasticity of the two body parts, that is, similar average elasticity. Table 2 summarizes the number of line segments expressed in each network structure shown in Figure 4 by texture feature. The smaller the number of lines, the simpler the feature's network structure, which can be interpreted as a texture feature that meaningfully distinguishes the elasticity of different body parts. According to Figure 4 and Table 2, mean had the lowest network complexity, and homogeneity had the highest.

4 | DISCUSSION

In this study, we attempted to establish an objective index that can predict elasticity without contact through image characteristics in the near-infrared band. According to previous research, aging of skin elasticity is closely related to the formation of skin wrinkles, and the relationship with skin elasticity has been analyzed using texture characteristics to objectify information about skin wrinkles. The results confirmed that the texture characteristics of the skin hyperspectral images in the near-infrared band and skin elasticity measured using a skin elastimeter had different relationships depending on the body part. It can be interpreted that the higher the correlation between texture and elasticity, the higher the possibility of measuring and predicting elasticity through texture features. If elasticity can

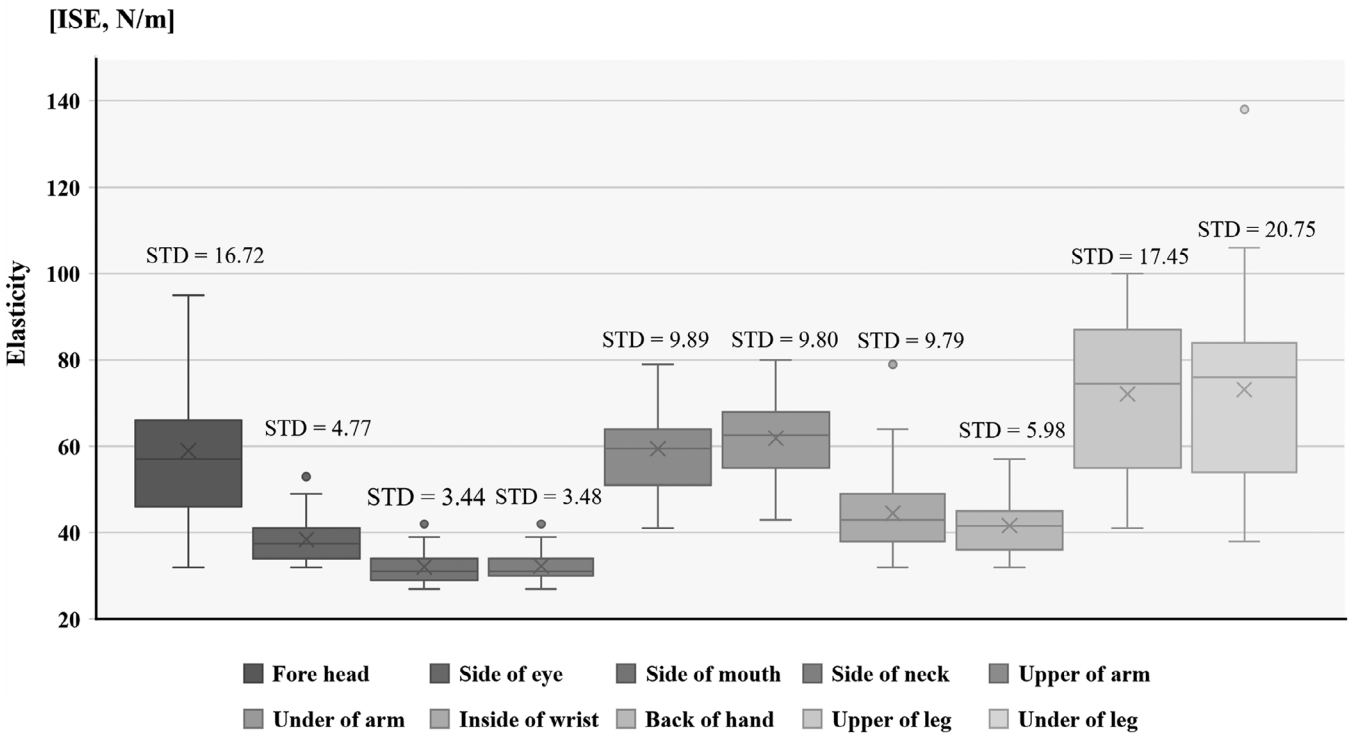

FIGURE 3 Comparison of elasticity averages by body part.

TABLE 1 Comparison of significant correlations between body parts and texture features.

	Section of body										
		Fore-head	Side of eye	Side of mouth	Side of neck	Upper of arm	Under of arm	Inside of wrist	Back of hand	Upper of leg	Under of leg
Feature of texture	Mean	N	Y(+)	N	N	Y(−)	Y(−)	Y(−)	N	Y(+)	Y(−)
	Std	N	Y(+)	Y(+)	N	Y(−)	Y(−)	N	N	N	Y(+)
	Entropy	Y(+)	Y(+)	Y(+)	N	Y(−)	Y(−)	N	N	N	Y(+)
	Contrast	N	Y(+)	N	N	N	Y(−)	N	N	N	Y(−)
	Correlation	N	Y(+)	Y(+)	Y(+)	N	Y(−)	N	N	N	Y(+)
	Homogeneity	N	Y(−)	N	N	N	Y(−)	N	N	N	Y(+)
	Energy	N	Y(−)	Y(−)	N	N	Y(+)	N	N	N	N

be predicted from the characteristics of skin images, an image-based, non-invasive, and non-contact skin elasticity measurement mechanism can be built without measuring elasticity by directly contacting the skin.

In the case of forehead, there was a significant positive correlation with entropy, indicating that the higher the amount of information about the forehead and pores in the forehead image in the unknown near-infrared band, the higher the elasticity value. In the case of side of neck, there was a significant positive correlation, which is considered to influence the formation of a higher elasticity value as the feature value of correlation, which is based on the fact that wrinkles are expressed in the diagonal direction due to the nature of the side of neck is higher. Inside of wrist negatively correlated with feature value of mean, indicating that the lower the average pixel value in the near-infrared band, the higher the elasticity value. Wrinkles that occur during frequent daily movements are expressed as low average pixel values in images in the near-infrared band, which can be interpreted as the formation of high elasticity. In the case of back of hand, there was no significant correlation with any feature. As back of hand is a part of the body with thin skin, it can be interpreted that there was no significant relationship between image characteristics and elasticity in the deeply penetrating near-infrared.[21] In the case of upper of leg, there was a significant positive correlation with the mean, indicating that upper of leg area was less affected by wrinkles as it moved down to the lower layer of the skin, and the resulting high average pixel value was interpreted to be related to the formation of high elasticity.

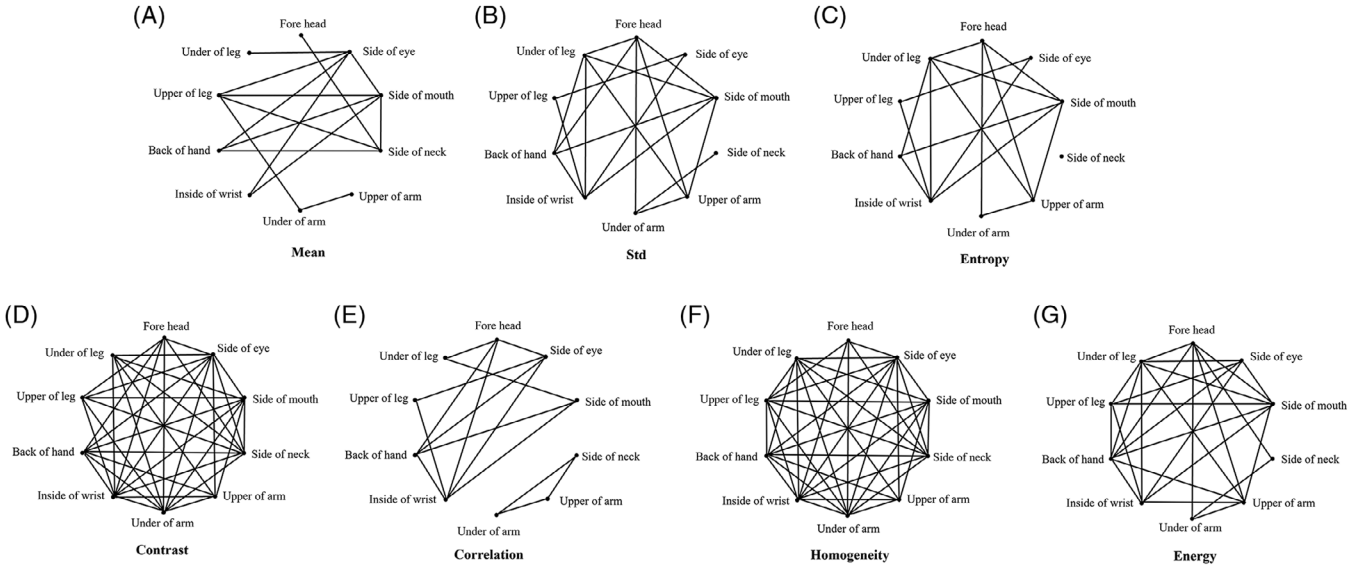

FIGURE 4 Elasticity similarity network between body parts by feature of texture. (A) Mean, (B) std., (C) entropy, (D) contrast, (E) correlation, (F) homogeneity, and (G) energy.

TABLE 2 Comparison of the number of line segments appearing in the relationship network for similar elastic body parts according to texture characteristics to evaluate significant elasticity average differences according to body parts by texture feature.

Feature of texture	Complexity (number of lines)
(a) Mean	14
(b) Std	18
(c) Entropy	16
(d) Contrast	37
(e) Correlation	15
(f) Homogeneity	40
(g) Energy	27

Different body parts have different elasticities, and the texture features that can be used to distinguish them well were selected in the following order: mean, correlation, entropy, std, energy, contrast, and homogeneity. The results showed that it was relatively difficult to distinguish skin elasticity according to body part based on the texture characteristics of the image in the near-infrared band, which proves that the light band that is highly relevant in determining skin elasticity is different for each body part.[22]

5 | CONCLUSSION

Overall, the skin image texture characteristics and skin elasticity in the near-infrared band showed different texture characteristics that were significantly correlated each body part. The image texture features in the near-infrared band were found significantly related to the elasticity of the side of the eye and under the arm. This confirms that the image texture features suitable for measuring and predicting skin elasticity may vary depending on the anatomical characteristics of the body. In the future, it will be necessary to research selecting light bands and texture characteristics suitable for observing skin elasticity at different body positions. Based on this research, the development of a system that can measure and predict skin elasticity in a non-contact manner can be expected in the future.

ACKNOWLEDGMENTS

This work was supported by the Soonchunhyang University Research Fund, BK21 FOUR (Fostering Outstanding Universities for Research) (5199990914048), the National Research Foundation of Korea (NRF) grant funded by the Korea government (MSIT) (2022R1A2C1010170), and Health Fellowship Foundation (2023).

CONFLICT OF INTEREST STATEMENT

The authors declare that there are no conflicts of interest.

DATA AVAILABILITY STATEMENT

The data that support the findings of this study are available on request from the corresponding author. The data are not publicly available due to privacy or ethical restrictions.

REFERNECES

1. Klinngam W, Rungkamoltip P, Thongin S, et al. Polymethoxyflavones from Kaempferia parviflora ameliorate skin aging in primary human dermal fibroblasts and ex vivo human skin. *Biomed Pharmacother*. 2022;145:112461. doi:10.1016/j.biopha.2021.112461
2. Bocheva G, Slominski RM, Janjetovic Z, et al. Protective role of melatonin and its metabolites in skin aging. *Int J Mol Sci*. 2022;23(3):1238. doi:10.3390/ijms23031238

3. Sharma A, Kuhad A, Bhandari R. Novel nanotechnological approaches for treatment of skin-aging. *J Tissue Viability*. 2022;31(3):374-386. doi:10.1016/j.jtv.2022.04.010
4. Yang CM, Xiang Z, Li ZL, Nan N, Wang XZ. Optical coherence elastography to evaluate depth-resolved elasticity of tissue. *Opt Express*. 2022;30(6):8709-8722. doi:10.1364/Oe.451704
5. Junker HJ, Thumm B, Halvachizadeh S, Mazza E. A quantitative comparison of devices for in vivo biomechanical characterization of human skin. *Mech Soft Mater*. 2023;5(1):5. doi:10.1007/s42558-023-00053-w
6. Choi JW, Kwon SH, Huh CH, Park KC, Youn SW. The influences of skin visco-elasticity, hydration level and aging on the formation of wrinkles: a comprehensive and objective approach. *Skin Res Technol*. 2013;19(1):E349-E355. doi:10.1111/j.1600-0846.2012.00650.x
7. Shao Y, Qin ZP, Wilks JA, et al. Physical properties of the photodamaged human skin dermis: rougher collagen surface and stiffer/harder mechanical properties. *Exp Dermatol*. 2019;28(8):914-921. 10.1111/exd.13728
8. Abbas DB, Lavin CV, Fahy EJ, et al. Standardizing dimensionless cutometer parameters to determine in vivo elasticity of human skin. *Adv Wound Care*. 2022;11(6):297-310. doi:10.1089/wound.2021.0082
9. Ryu HS, Joo YH, Kim SO, Park KC, Youn SW. Influence of age and regional differences on skin elasticity as measured by the cutometer (R). *Skin Res Technol*. 2008;14(3):354-358. doi:10.1111/j.1600-0846.2008.00302.x
10. Kirby M, Tang PJ, Liou HC, et al. Probing elastic anisotropy of human skin in vivo with light using non-contact acoustic micro-tapping OCE and polarization sensitive OCT. *Sci Rep-Uk*. 2022;12(1):3963. doi:10.1038/s41598-022-07775-3
11. Finlayson L, Barnard IRM, McMillan L, et al. Depth penetration of light into skin as a function of wavelength from 200 to 1000 nm. *Photochem Photobiol*. 2022;98(4):974-981. doi:10.1111/php.13550
12. Shimojo Y, Nishimura T, Hazama H, Ozawa T, Awazu K. Measurement of absorption and reduced scattering coefficients in Asian human epidermis, dermis, and subcutaneous fat tissues in the 400- to 1100-nm wavelength range for optical penetration depth and energy deposition analysis . *J Biomed Opt*. 2021;26(1):019802. doi:10.1117/1.Jbo.26.1.019802
13. Manojlovic T, Tomanic T, Stajduhar I, Milanic M. Rapid extraction of skin physiological parameters from hyperspectral images using machine learning. *Appl Intell*. 2023;53(13):16519-16539. doi:10.1007/s10489-022-04327-0
14. Mahmoud A, El-Sharkawy YH. Quantitative phase analysis and hyperspectral imaging for the automatic identification of veins and blood perfusion maps. *Photodiagn Photodyn*. 2023;42:103307. doi:10.1016/j.pdpdt.2023.103307
15. Calin MA, Parasca SV, Calin MR, Petrescu E. An analysis of human dorsal hand skin texture using hyperspectral imaging technique for assessing the skin aging process. *Appl Spectrosc*. 2017;71(3):391-400. doi:10.1177/0003702816659667
16. Ivanova Z, Aleksiev T, Dobrev H, Atanasov N. Use of a novel indentometer to evaluate skin stiffness in healthy and diseased human skin. *Skin Res Technol*. 2023;29(7):e13384. doi:10.1111/srt.13384
17. Viren T, Iivarinen JT, Sarin JK, Harvima I, Mayrovitz HN. Accuracy and reliability of a hand-held in vivo skin indentation device to assess skin elasticity. *Int J Cosmetic Sci*. 2018;40(2):134-140. doi:10.1111/ics.12444
18. Cios A, Ciepielak M, Szymanski L, et al. Effect of different wavelengths of laser irradiation on the skin cells. *Int J Mol Sci*. 2021;22(5):2437. doi:10.3390/ijms22052437
19. Sorbellini E, Rucco M, Rinaldi F. Photodynamic and photobiological effects of light-emitting diode (LED) therapy in dermatological disease: an update. *Laser Med Sci*. 2018;33(7):1431-1439. doi:10.1007/s10103-018-2584-8
20. Park BE, Jang WS, Yoo SK. Texture analysis of supraspinatus ultrasound image for computer aided diagnostic system. *Healthc Inform Res*. 2016;22(4):299-304. doi:10.4258/hir.2016.22.4.299
21. Sandby-Moller J, Poulsen T, Wulf HC. Epidermal thickness at different body sites: relationship to age, gender, pigmentation, blood content, skin type and smoking habits. *Acta Derm-Venereol*. 2003;83(6):410-413. doi:10.1080/00015550310015419
22. Setchfield K, Gorman A, Simpson A, Somekh MG, Wright AJ. Relevance and utility of the in-vivo and ex-vivo optical properties of the skin reported in the literature: a review [Invited]. *Biomed Opt Express*. 2023;14(7):3555-3583. doi:10.1364/Boe.493588

How to cite this article: Kim J, Lee O. Correlation analysis between texture features and elasticity of skin hyperspectral images in the near-infrared band. *Skin Res Technol*. 2024;30:e13654. https://doi.org/10.1111/srt.13654